Transport in ferromagnetic $GdTiO_3/SrTiO_3$ heterostructures

Pouya Moetakef,[1] Jack Y. Zhang,[1] Alexander Kozhanov,[2] Bharat Jalan,[1] Ram Seshadri,[1] S. James Allen,[2] and Susanne Stemmer[1,a)]
[1]*Materials Department, University of California, Santa Barbara, California 93106-5050, USA*
[2]*Department of Physics, University of California, Santa Barbara, California 93106-9530, USA*

(Received 10 February 2011; accepted 28 February 2011; published online 17 March 2011)

Epitaxial $GdTiO_3/SrTiO_3$ structures with different $SrTiO_3$ layer thicknesses are grown on (001) $(LaAlO_3)_{0.3}(Sr_2AlTaO_6)_{0.7}$ substrate surfaces by hybrid molecular beam epitaxy. It is shown that the formation of the pyrochlore ($Gd_2Ti_2O_7$) phase can be avoided if $GdTiO_3$ is grown by shuttered growth, supplying alternating monolayer doses of Gd and of the metalorganic precursor that supplies both Ti and O. Phase-pure $GdTiO_3$ films grown by this approach exhibit magnetic ordering with a Curie temperature of 30 K. The electrical transport characteristics can be understood as being dominated by a conductive interface layer within the $SrTiO_3$. © *2011 American Institute of Physics*. [doi:10.1063/1.3568894]

Heterostructures with interfaces between band insulators, such as $SrTiO_3$ or $LaAlO_3$, and Mott–Hubbard insulators, such as $LaTiO_3$, have recently attracted attention for tailoring the wide range of emergent phenomena that are associated with strong electron correlations.[1–5] While many studies have focused on $LaTiO_3$, other rare earth titanates ($RTiO_3$, where R is a trivalent rare earth ion) offer additional functionalities, such as ferromagnetism.[6,7] In $GdTiO_3$, for example, the Ti magnetic moments order ferromagnetically and couple antiparallel to the ferromagnetic component of the Gd sites, giving rise to net ferrimagnetism below a Curie temperature of ~30 K.[6] Growth of epitaxial rare earth titanates is challenging because of the low oxygen partial pressures that are needed to stabilize Ti in a +3 valence state. Oxygen-excess [likely more accurately described as cation-deficiency or $R_{1-x}Ti_{1-y}O_3$ (Ref. 8)] closes the Mott–Hubbard band gap and the magnetic ordering disappears.[9,10] Intergrowth of the pyrochlore phase ($R_2Ti_2O_7$) is commonly observed under oxygen-rich conditions.[4,11] In this Letter we show that phase-pure, epitaxial, ferromagnetic $GdTiO_3/SrTiO_3$ heterostructures with a Curie temperature close to that of bulk $GdTiO_3$ can be grown by molecular beam epitaxy (MBE). The electrical properties indicate contributions from a conductive interface layer in the $SrTiO_3$.

$GdTiO_3/SrTiO_3$ heterostructures were grown on (001) surfaces of $(LaAlO_3)_{0.3}(Sr_2AlTaO_6)_{0.7}$ (LSAT) single crystals with Ta-backing layers in a GEN930 oxide MBE system (Veeco, St. Paul, Minnesota) with a chamber background pressure of 10^{-9} torr. A hybrid MBE approach with both gas and solid sources was used.[12] To supply Ti, titanium tetra isopropoxide (TTIP, 99.999% SAFC Hitech, St. Louis, MO) was evaporated, which also served as the source for oxygen.[13] Strontium (99.95%, Sigma Aldrich APL, Urbana, Illinois) and Gd (99.99%, Ames MPC, Ames, Iowa) were evaporated from effusion cells. The substrate temperature was 950 °C (thermocouple temperature). Epitaxial $SrTiO_3$ layers with different thicknesses were grown by codeposition, as described elsewhere.[12] $GdTiO_3$ was deposited using shuttered growth with alternating monolayer doses of TTIP and Gd. All $GdTiO_3$ films in this study were ~19 nm (50 pseudocubic unit cells). No additional oxygen was supplied during either $SrTiO_3$ or $GdTiO_3$ growth. This was necessary to avoid the formation of $Gd_2Ti_2O_7$ but resulted in oxygen-deficient $SrTiO_3$. Furthermore, codeposition of Gd and TTIP using similar beam flux ratios also resulted in $Gd_2Ti_2O_7$. A possible reason why shuttered growth assists in stabilizing the $GdTiO_3$ phase is that it allows for desorption of excess oxygen from the TTIP precursor before Gd is deposited. Films grown directly on LSAT without a $SrTiO_3$ buffer layer were amorphous. For scanning transmission electron microscopy (STEM) characterization, samples were capped with $SrTiO_3$ as uncapped samples were too sensitive to moisture to survive sample preparation. The magnetization as a function of temperature and magnetic field was measured in a Quantum Design (San Diego, California) Magnetic Properties Measurement System. Four-point probe sheet resistances and Hall coefficients as a function of temperature were measured using a Physical Properties Measurement System (Quantum Design PPMS) in Van der Pauw geometry with 40 nm Al/20 nm Ni/150 nm Au Ohmic contacts deposited by e-beam evaporation and wire bonded using a gold wire.

Figure 1(a) shows a θ-2θ radial x-ray diffraction (XRD) scan of a $GdTiO_3/SrTiO_3/LSAT$ heterostructure, showing $hk0$-type reflections of $GdTiO_3$ and the $00l$ reflections of the LSAT substrate. Bulk $GdTiO_3$ is orthorhombic with lattice parameters a=5.407 Å, b=5.667 Å, and c=7.692 Å,[9,14] while LSAT has a cubic structure with a=7.736 Å.[15] Therefore, $GdTiO_3$ (GTO) films may grow with $(001)_{GTO}$ or $(110)_{GTO}$ parallel to $(001)_{LSAT}$, respectively. The latter orientation has a smaller lattice mismatch. The out-of-plane lattice spacing measured in high-resolution XRD [3.921 Å, see inset in Fig. 1(a)] is very close to the out-of-plane $(110)_{GTO}$ plane spacing (3.924 Å), estimated from the elastic constants[16] and bulk lattice parameters, assuming that the $GdTiO_3$ film is strained in-plane to match the LSAT lattice parameter. Thickness fringes indicate a smooth surface and coherent growth. The high-angle annular dark-field (HAADF) STEM image shown in Fig. 1(b) confirms the epitaxial relationship, chemically abrupt interface and the absence of pyrochlore-type and other extended defects.

The magnetization as a function of temperature is shown in Fig. 2(a) for a heterostructure with 1.2 nm $SrTiO_3$. A

a)Electronic mail: stemmer@mrl.ucsb.edu.

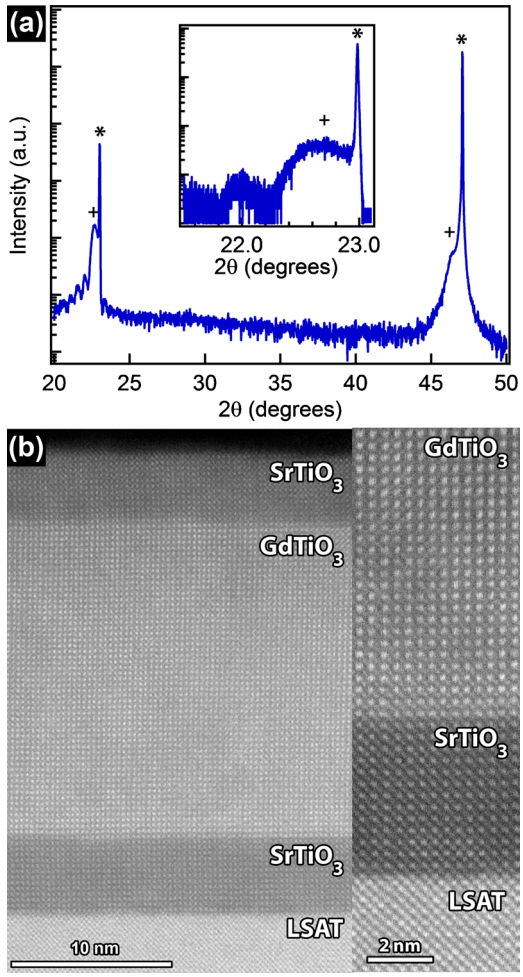

FIG. 1. (Color online) (a) θ-2θ XRD scan of $GdTiO_3/SrTiO_3$ grown on (001) LSAT. The thickness of the $SrTiO_3$ buffer layer was about 1.2 nm. The inset shows a high resolution θ-2θ XRD scan around the 001 LSAT reflection. The LSAT reflections are labeled with asterixes and the $GdTiO_3$ reflections with crosses. (b) Cross-section HAADF/STEM image (corrected for drift) of a 19 nm $GdTiO_3$ film with 5 nm $SrTiO_3$ buffer and cap, respectively. The $GdTiO_3$ layer appears brighter than the $SrTiO_3$ because of the strong atomic number sensitivity of the HAADF imaging mode.

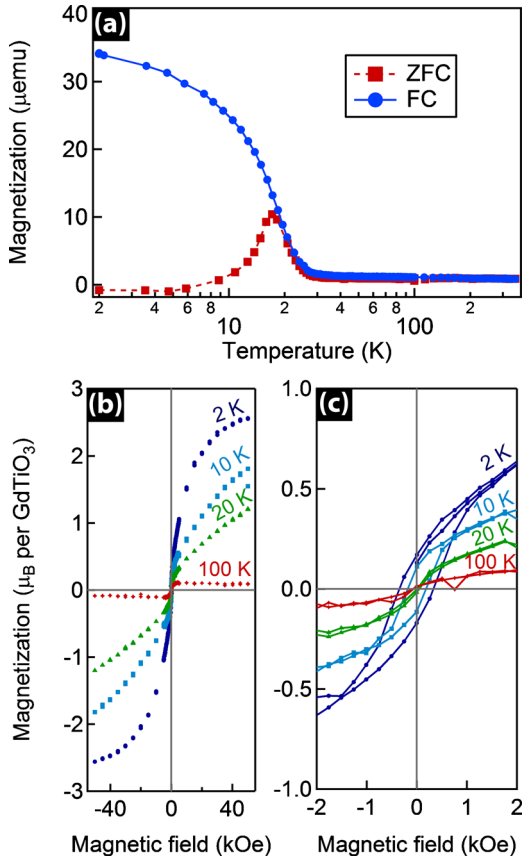

FIG. 2. (Color online) Magnetic properties of 19 nm $GdTiO_3$/1.2 nm $SrTiO_3$ on LSAT with 350 nm Ta backing layer, measured with the magnetic field parallel to the substrate surface. (a) Magnetization as a function of temperature measured with a magnetic field of 100 Oe applied during heating, zero field cooled (ZFC) and field cooled (FC). [(b) and (c)] Magnetization as a function of magnetic field after subtraction of the linear diamagnetic signal for different temperatures between 2 to 100 K.

transition from paramagnetism to magnetic ordering occurs around 30 K. Figures 2(b) and 2(c) show the magnetization as a function of magnetic field after subtraction of the diamagnetic and paramagnetic signal at 100 K. A ferromagnetic hysteresis appears at low temperatures [Fig. 2(c)]. The Curie temperature (T_c) of 30 K and the small remanence and coercitivity are similar to bulk $GdTiO_3$.[6] Because the magnetic ordering disappears for nonstoichiometric $R_{1-x}Ti_{1-y}O_3$,[9] the results suggest that the films are reasonably close to stoichiometry. The magnetic properties of a sample with a thicker (44 nm) $SrTiO_3$ layer, which are more conductive, are similar, consistent with the fact that the magnetism is due to the $GdTiO_3$ layer and the conduction dominated by a space charge layer in the $SrTiO_3$ (see below).

Figure 3 shows the sheet resistance as a function of temperature for samples with different $SrTiO_3$ buffer layer thickness. The Hall coefficients are negative for all samples, indicating that electrons are the dominant charge carriers with sheet carrier densities of $\sim 3 \times 10^{14}$ cm^{-2}. However, caution should be applied because Hall coefficients cannot be easily converted into carrier densities if more than one type of carrier is present, which may be the case here. For samples with $SrTiO_3$ layer thicknesses between 1.2 and 5 nm, the weak temperature dependence and strong signature of weak localization at low temperatures[17] is consistent with transport at the critical conductance at the transition to localization. Samples with thicker buffer layers are metallic: they

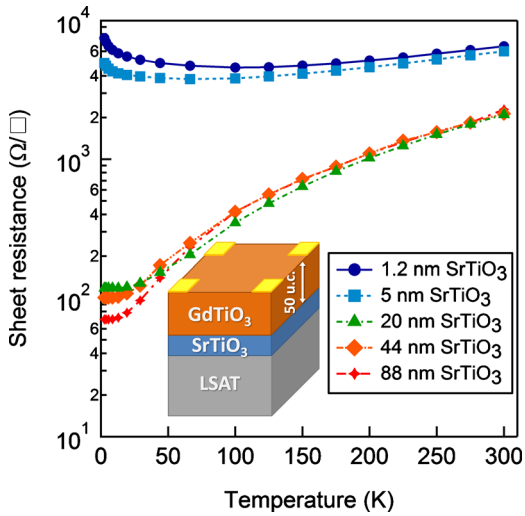

FIG. 3. (Color online) Sheet resistance as a function of temperature for 19 nm $GdTiO_3$ grown on LSAT with different $SrTiO_3$ buffer layer thicknesses ranging from 1.2 to 88 nm.

have much lower sheet resistance and exhibit resistance ratios greater ~20, with a resistance decrease with temperature that is largely due to the increase in the mobility. As mentioned above, under these growth conditions, the $SrTiO_3$ layers should be oxygen deficient and metallic[18] and a continuous decrease in sheet resistance with increasing $SrTiO_3$ layer thickness would be expected. The results in Fig. 3 show, however, that the sheet resistance remains constant for $SrTiO_3$ buffer layers thicker than 20 nm. Despite the very reducing growth conditions, the results are thus consistent with the formation of an interfacial conductive layer at the $SrTiO_3/GdTiO_3$ interface rather than uniform conduction throughout the $SrTiO_3$. The upper thickness limit for this layer is 20 nm and relatively high mobilities around $\sim 200-300\ cm^2\ V^{-1}\ s^{-1}$ (at 2 K) suggest that the conductive layer resides in the $SrTiO_3$. Further studies are necessary to determine the origins of the interfacial conductive layer, which will require knowledge of the precise band lineups at the interface and of the influence of interfacial charge, such as may arise from the valence state mismatch between Sr and Gd at the interface.[19,20]

In summary, we have shown that epitaxial $GdTiO_3/SrTiO_3$ heterostructures with phase-pure $GdTiO_3$ can be grown using a shuttered hybrid MBE approach. The magnetic properties are in good agreement with those of bulk, stoichiometric $GdTiO_3$. The electrical transport shows contributions from an interfacial conductive layer in the $SrTiO_3$. These heterostructures offer a wide range of opportunities for tailoring the magnetic properties of strongly correlated materials.

P.M. and J.Y.Z. were supported through awards from the U.S. National Science Foundation (Grant No. DMR-1006640) and DOE Basic Energy Sciences (Grant No. DE-FG02-02ER45994). S.S. and S.J.A. acknowledge support through a MURI program of the Army Research Office (Grant No. W911-NF-09-1-0398). B.J. is supported by the MRSEC Program of the National Science Foundation (Award No. DMR 05-20415). The work made use of the UCSB Nanofabrication Facility, a part of the NSF-funded NNIN network.

[1]A. Ohtomo, D. A. Muller, J. L. Grazul, and H. Y. Hwang, Nature (London) **419**, 378 (2002).
[2]S. Okamoto and A. J. Millis, Nature (London) **428**, 630 (2004).
[3]M. Takizawa, H. Wadati, K. Tanaka, M. Hashimoto, T. Yoshida, A. Fujimori, A. Chikamatsu, H. Kumigashira, M. Oshima, K. Shibuya, T. Mihara, T. Ohnishi, M. Lippmaa, M. Kawasaki, H. Koinuma, S. Okamoto, and A. J. Millis, Phys. Rev. Lett. **97**, 057601 (2006).
[4]K. S. Takahashi, M. Onoda, M. Kawasaki, N. Nagaosa, and Y. Tokura, Phys. Rev. Lett. **103**, 057204 (2009).
[5]J. S. Kim, S. S. A. Seo, M. F. Chisholm, R. K. Kremer, H. U. Habermeier, B. Keimer, and H. N. Lee, Phys. Rev. B **82**, 201407 (2010).
[6]H. D. Zhou and J. B. Goodenough, J. Phys.: Condens. Matter **17**, 7395 (2005).
[7]G. Amow, J. S. Zhou, and J. B. Goodenough, J. Solid State Chem. **154**, 619 (2000).
[8]D. A. Crandles, T. Timusk, J. D. Garrett, and J. E. Greedan, Phys. Rev. B **49**, 16207 (1994).
[9]A. C. Komarek, H. Roth, M. Cwik, W. D. Stein, J. Baier, M. Kriener, F. Bouree, T. Lorenz, and M. Braden, Phys. Rev. B **75**, 224402 (2007).
[10]M. Imada, A. Fujimori, and Y. Tokura, Rev. Mod. Phys. **70**, 1039 (1998).
[11]A. Ohtomo, D. A. Muller, J. L. Grazul, and H. Y. Hwang, Appl. Phys. Lett. **80**, 3922 (2002).
[12]B. Jalan, R. Engel-Herbert, N. J. Wright, and S. Stemmer, J. Vac. Sci. Technol. A **27**, 461 (2009).
[13]B. Jalan, R. Engel-Herbert, J. Cagnon, and S. Stemmer, J. Vac. Sci. Technol. A **27**, 230 (2009).
[14]D. A. MacLean, H.-N. Ng, and J. E. Greedan, J. Solid State Chem. **30**, 35 (1979).
[15]D. J. Tao, H. X. Wu, X. D. Xu, R. S. Yan, F. Y. Liu, A. P. B. Sinha, X. P. Jiang, and H. L. Hu, Opt. Mater. **23**, 425 (2003).
[16]B. Steele, A. D. Burns, A. Chernatynskiy, R. W. Grimes, and S. R. Phillpot, J. Mater. Sci. **45**, 168 (2010).
[17]See supplementary material at http://dx.doi.org/10.1063/1.3568894 for the magnetoresistance as a function of $SrTiO_3$ buffer layer thickness.
[18]H. P. R. Frederikse and W. R. Hosler, Phys. Rev. **161**, 822 (1967).
[19]H. Kroemer, Surf. Sci. **132**, 543 (1983).
[20]J. Mannhart, D. H. A. Blank, H. Y. Hwang, A. J. Millis, and J. M. Triscone, MRS Bull. **33**, 1027 (2008).